

Quantum Monte Carlo study of a one-dimensional phase-fluctuating condensate in a harmonic trap

C. Gils,¹ L. Pollet,¹ A. Vernier,² F. Hebert,² G.G. Batrouni,² and M. Troyer¹

¹*Institut für Theoretische Physik, ETH Zürich, CH-8093 Zürich, Switzerland*

²*Institute Non-Linéaire de Nice, UMR CNRS 6618,*

Université de Nice-Sophia Antipolis, 1361 route des Lucioles, F-06560 Valbonne, France

(Dated: June 11, 2018)

We study numerically the low-temperature behavior of a one-dimensional Bose gas trapped in an optical lattice. For a sufficient number of particles and weak repulsive interactions, we find a clear regime of temperatures where density fluctuations are negligible but phase fluctuations are considerable, i.e., a quasicondensate. In the weakly interacting limit, our results are in very good agreement with those obtained using a mean-field approximation. In coupling regimes beyond the validity of mean-field approaches, a phase-fluctuating condensate also appears, but the phase-correlation properties are qualitatively different. It is shown that quantum depletion plays an important role.

PACS numbers: 03.75.Hh, 03.75.Lm, 05.30.Jp

In a spatially homogeneous one-dimensional (1D) gas of bosons, spontaneous symmetry breaking is excluded at all temperatures T [1, 2, 3]. Long-range order is absent in this system due to the fluctuations of the phase of the order parameter, as seen in the asymptotic decay of the equal-time single-particle Green's function (algebraic for $T = 0$ and exponential for $T > 0$) [4, 5, 6, 7]. However, analytical studies of trapped 1D Bose gases with a fixed particle number, N , reveal new phenomena. For example, the ground state of a noninteracting 1D Bose gas in a harmonic trap with frequency ω becomes macroscopically populated below a temperature $T_c \simeq N\hbar\omega/\ln(2N)$, i.e., a Bose-Einstein condensate (BEC) exists in the finite system [8]. Several mean-field studies indicate that weak repulsive interactions introduce an additional effect, namely, that fluctuations of the density are suppressed at low temperatures, and a phase-fluctuating condensate, or quasicondensate, appears [9, 10, 11, 12, 13, 14]; for the homogeneous system see [15]. Roughly speaking, this is a regime in temperature where the distribution of particles in space is given by a temperature-independent Thomas-Fermi profile, while thermal fluctuations of the phase are present and lead to a phase-coherence length that is smaller than the condensate cloud. Only below a much lower temperature do phase fluctuations also become negligible and phase coherence extends over the complete condensate cloud. A phase-fluctuating condensate emerges only in low dimensions and has been experimentally observed in sufficiently anisotropic 3D trapping geometries [16].

In this paper, we verify the existence of a 1D quasicondensate, on trapped optical lattices, starting from a microscopic approach whose validity is not restricted to certain parameter regimes. Using quantum-Monte Carlo simulations of the Bose-Hubbard model, we investigate the properties of the phase-fluctuating condensate for various choices of interaction strength and density. For

weak interactions, our results are in excellent agreement with mean-field estimates in the continuum [10]. In an intermediate-coupling regime beyond the weakly interacting limit, but not yet in the strong-coupling domain, the quasicondensate regime spreads over an even larger temperature range. Nonetheless, we observe qualitatively different phase-correlation properties which do not follow from existing analytical approaches.

First, we briefly review the notion of a quasicondensate (QC) in a weakly interacting (WI) 1D trapped Bose gas as presented in [10]. In the WI limit, we have $\gamma = mg/\hbar^2 n \ll 1$, where n is the average particle density, m the particle mass, and g the coupling constant of a repulsive contact interaction [17]. In second-quantized representation, the Hamiltonian of the system is given by

$$\hat{H} = \int dz \hat{\psi}^\dagger(z) \left(-\frac{\hbar^2 \nabla^2}{2m} + V_t(z) + \frac{g}{2} \hat{\psi}^\dagger(z) \hat{\psi}(z) \right) \hat{\psi}(z), \quad (1)$$

where $\hat{\psi}(z)$ is the bosonic field operator and $V_t(z) = m\omega^2 z^2/2$ the external trapping potential centered at the origin. The authors in [10] show that density fluctuations $\langle \delta \hat{n}(z) \delta \hat{n}(z') \rangle$, where $\hat{n}(z) = n(z) + \delta \hat{n}(z)$, are suppressed for inverse temperatures $\beta \gg \beta_d = (N\hbar\omega)^{-1}$ (Boltzmann constant $k_B = 1$). The field operator can then be expressed as $\hat{\psi}(z) = \sqrt{n(z)} \exp[i\hat{\phi}(z)]$. Thermal fluctuations of the phase are evident from the decay of the one-particle density matrix, or (equal-time) Green's function, which is obtained as [10]

$$\langle \hat{\psi}^\dagger(z) \hat{\psi}(z') \rangle = \sqrt{n(z)n(z')} \exp(-\langle \delta \hat{\phi}_{zz'}^2 \rangle / 2), \quad (2a)$$

where $\delta \hat{\phi}_{zz'}^2 = (\hat{\phi}(z) - \hat{\phi}(z'))^2$, and

$$\langle \delta \hat{\phi}_{zz'}^2 \rangle = \frac{4\beta_d \mu_{\text{TF}}}{3\beta \hbar \omega} \left| \ln \left(\frac{(L_{\text{TF}} - z')}{(L_{\text{TF}} + z')} \frac{(L_{\text{TF}} + z)}{(L_{\text{TF}} - z)} \right) \right|, \quad (2b)$$

where $\mu_{\text{TF}} = (3Ng/4)^{2/3} (m\omega^2/2)^{1/3}$ is the chemical potential, and $L_{\text{TF}} = \sqrt{2\mu_{\text{TF}}/m\omega^2}$ the half size of the

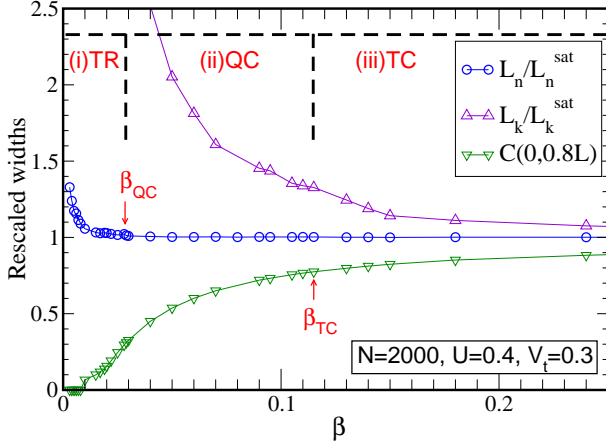


FIG. 1: (Color online) (i) Thermal regime: As a result of both density and phase fluctuations, the widths of the density profile, L_n , and the momentum profile, L_k , depend on β with $L_n(\beta) > L_n^{\text{sat}}$, $L_k(\beta) > L_k^{\text{sat}}$. (ii) Quasicondensate: Density fluctuations are negligible ($L_n = L_n^{\text{sat}}$, L is the half size of the condensate cloud for $\beta \geq \beta_{\text{QC}}$). However, the phase fluctuates, as seen for $L_k(\beta) > L_k^{\text{sat}}$, phase correlation function $C(0,0.8L) < 1$. (iii) True condensate: Phase fluctuations also disappear as $L_k(\beta)$ approaches L_k^{sat} , and $C(0,0.8L)$ approaches 1. The numerical results are $\beta_{\text{QC}} \approx 0.03$ and $\beta_{\text{TC}} = 0.115(5)$ (analytical estimate: $\beta_{\text{TC}} = 0.116$).

condensate in the Thomas-Fermi (TF) approximation ($\mu_{\text{TF}} \gg \hbar\omega$; see e.g. [19]). For $\beta \rightarrow \infty$, it follows from Eq. (2b) that $\langle \delta\phi_{zz'}^2 \rangle \rightarrow 0$, and thus $G(z, z') \rightarrow \sqrt{n(z)n(z')}$, i.e. the system is completely phase coherent.

As is well known [18], the discretization of Eq. (1) yields the Bose-Hubbard model with lattice Hamiltonian

$$\hat{H} = -J \sum_{\langle j, j' \rangle} (\hat{a}_j^\dagger \hat{a}_{j'} + \text{H.c.}) + \frac{U}{2} \sum_j \hat{n}_j (\hat{n}_j - 1) + V_t \sum_j (j - M/2)^2 \hat{n}_j, \quad (3)$$

where \hat{a}_j^\dagger creates a particle at optical lattice site j and $\hat{n}_j = \hat{a}_j^\dagger \hat{a}_j$. The number of lattice sites M is chosen such that the occupation at the boundaries of the lattice is zero. We work in units where the lattice spacing and $\hbar^2/2m$ are set to 1. In these units, parameters in Eqs. (1) and (3) are related as follows: $J = 1$, $U = g$, $V_t = (\hbar\omega)^2/4$. Our system is defined on an optical lattice, however, in the WI and degenerate limits, the discrete and continuum description of the phase-fluctuating condensate are equivalent [12]. We investigate this model using a worm update quantum Monte Carlo (QMC) method in the canonical ensemble [20]. This nonlocal update scheme allows for an efficient evaluation of the equal-time Green's function $G(j, j') = \langle \hat{a}_j^\dagger \hat{a}_{j'} \rangle$. Phase correlation properties are also apparent from the shapes of the momentum profile, $n(k) = \sum_{j, j'} G(j, j') \exp[ik(j - j')]$,

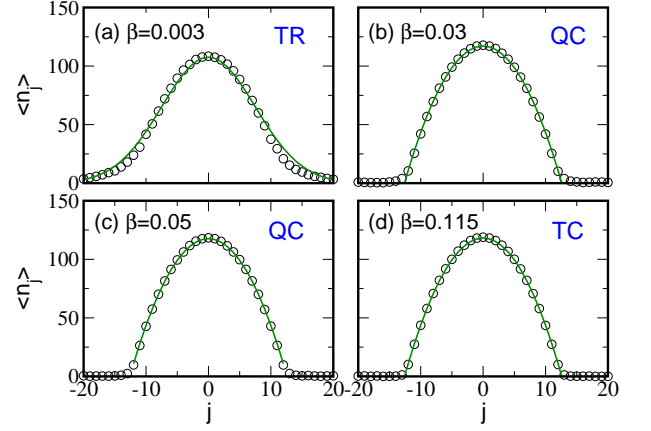


FIG. 2: (Color online) $N = 2000$, $U = 0.4$, $V_t = 0.3$ ($\gamma = 0.003$). Density fluctuations are suppressed for $\beta \geq \beta_{\text{QC}} \approx 0.03$ and the density profiles $n_j = \langle \hat{n}_j \rangle$ (o) are identical for $\beta \geq \beta_{\text{QC}}$ (b)-(d). In (a), the line is a fit to a Gaussian profile, while in (b)-(d) the lines are fits to a TF profile $n_0(1 - j^2/L^2)$ where $L = 12.6$ ($L_{\text{TF}} = 12.6$). Error bars in the figures are always smaller than the symbol size.

and the rescaled Green's function (phase correlation function), $C(j, j') = G(j, j') / \sqrt{n_j n_{j'}}$, where $n_j = \langle \hat{n}_j \rangle$ is the density distribution. In the WI, TF and mean-field (N large enough) limits, we observe three different regimes in temperature: the thermal regime (TR), the quasicondensate (QC) and the “true condensate” (TC). These regimes are separated by smooth crossovers, which are characterized by the temperatures $1/\beta_{\text{QC}}$ and $1/\beta_{\text{TC}}$. We discuss the properties of the three regimes and compare our results with the mean-field results listed above. Furthermore, we consider the emergence of the phase-fluctuating condensate depending on the choice of parameters N , U and V_t , including parameter sets that are beyond the WI limit.

In the thermal regime $\beta < \beta_{\text{QC}}$, both the density and the phase are governed by thermal fluctuations. Hence, all quantities exhibit a strong temperature dependence. The width of the density profile, $L_n(\beta)$ (standard deviation of n_j), decreases throughout the TR, until it reaches its minimum value L_n^{sat} at the inverse temperature β_{QC} , as shown in Fig. 1. The shape of the density profile is approximately Gaussian, which is expected for high temperatures where the bosonic nature of the particles becomes less relevant [Fig. 2 (a)]. The strong phase fluctuations are seen in the width of the momentum profile, $L_k(\beta)$ [standard deviation of $n(k)$], which is much larger than its minimum value L_k^{sat} [Fig. 1], as well as in the exponential decay of the Green's function [Fig. 3 (a)]. We recall that there exists no analytical estimate for β_{QC} ; density fluctuations are merely predicted to become small for $\beta \gg \beta_d = (4V_t N^2)^{-1/2}$ [10]. For the parameter set in the Figs. 1-3, we have $\beta_d \approx 0.02\beta_{\text{QC}}$.

In the quasicondensate ($\beta_{\text{QC}} \leq \beta < \beta_{\text{TC}}$), the density

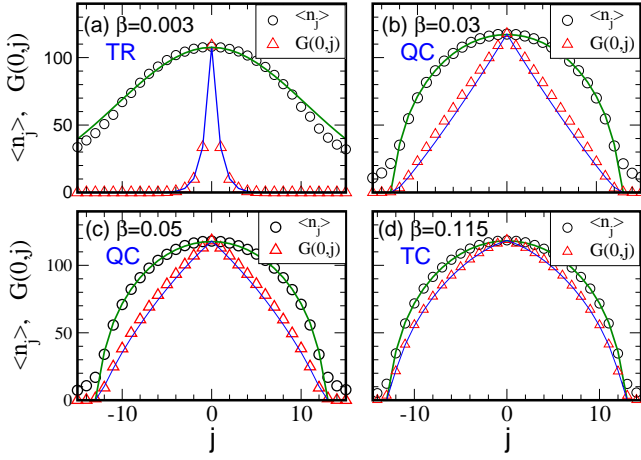


FIG. 3: (Color online) $N = 2000$, $U = 0.4$, $V_t = 0.3$. The density profiles $\sqrt{n_0 n_j}$ (\circ) are virtually independent of temperature for $\beta \geq \beta_{QC} \approx 0.03$ (b)-(d), while the Green's function $G(0, j)$ (\triangle) varies with β . The lines are the analytical estimates, a Gaussian fit for $\sqrt{n_0 n_j}$ in (a), a TF profile $n_0 \sqrt{1 - j^2/L^2}$ for $\sqrt{n_0 n_j}$ in (b)-(d) and $\sqrt{n_0 n_j} \exp(-\alpha |\ln[(L - j)/(L + j)]|)$ [see Eq. (2)] for $G(0, j)$.

no longer fluctuates: the density profiles n_j at different temperatures $\beta \geq \beta_{QC}$ are identical and in excellent agreement with a TF inverse parabola shape of half size L , where L equals to L_{TF} [Figs. 2(b)- 2(d)]. However, thermal fluctuations of the phase are considerable. Thus, the width of the momentum profile, and the phase correlation function still change with decreasing temperature (Fig. 1). Figures 3(b)- 3(d) demonstrate that the Green's function varies substantially for different $\beta \geq \beta_{QC}$, while the density profile $\sqrt{n_0 n_j}$ is invariant. We find very good agreement with the mean-field result Eq. (2): the ansatz $\sqrt{n_0 n_j} \exp\{-\alpha |\ln[(L - j)/(L + j)]|\}$, with α a fitting parameter, reproduces $G(0, j)$ (Fig. 3).

At temperatures much lower than $1/\beta_{QC}$, phase fluctuations also become suppressed. Therefore, it is meaningful to introduce a second crossover temperature, $1/\beta_{TC}$, to a phase-coherent regime, the true condensate. We define β_{TC} as the temperature where $C(0, 0.8L) = \exp(-0.25)$. This definition is somewhat arbitrary, but yields a scale below which the system can safely be considered to be phase-coherent. In addition, it allows for a comparison of analytical and numerical results, with the analytical equivalent of β_{TC} being $\tilde{\beta}_{TC} = 4\beta_d \mu_{TF} \ln(9)/3\hbar\omega$ [which is the temperature where $\langle \delta \hat{\phi}_{0z'}^2 \rangle = 0.5$ for $|z'| = 0.8L_{TF}$; see Eq. 2]. Note that the true condensate is not to be confused with a BEC, and strictly only appears at zero temperature (Thomas-Fermi condensate; see [10]). In the true condensate, the Green's function and the momentum profile approach their temperature-independent ground state shapes, as shown by the convergence of

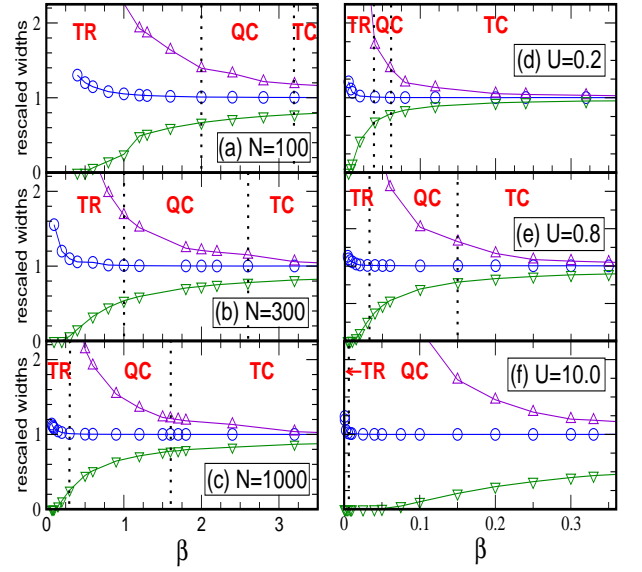


FIG. 4: (Color online) The size $s = \beta_{TC}/\beta_{QC}$, of the QC regime depending on the number of particles N (a - c, $U = 0.5$, $V_t = 0.01$) and coupling constant U (d - f, $N = 2000$, $V_t = 0.4$).

L_n/L_n^{sat} (\circ), L_k/L_k^{sat} (\triangle), $C(0, 0.8L)$ (∇)
a) $\gamma = 0.08$, $\tilde{\beta}_{TC} = 3.5$, $\beta_{TC} \approx 3.2(4)$, $\beta_{QC} \approx 2.0$, $s \approx 1.6$
b) $\gamma = 0.04$, $\tilde{\beta}_{TC} = 2.5$, $\beta_{TC} \approx 2.6(4)$, $\beta_{QC} \approx 1.0$, $s \approx 2.6$
c) $\gamma = 0.02$, $\tilde{\beta}_{TC} = 1.64$, $\beta_{TC} \approx 1.6(1)$, $\beta_{QC} \approx 0.3$, $s \approx 5.3$
d) $\gamma = 0.001$, $\tilde{\beta}_{TC} = 0.06$, $\beta_{TC} \approx 0.06(2)$, $\beta_{QC} \approx 0.04$, $s \approx 1.5$
e) $\gamma = 0.006$, $\tilde{\beta}_{TC} = 0.15$, $\beta_{TC} \approx 0.15(5)$, $\beta_{QC} \approx 0.03$, $s \approx 5$
f) $\gamma = 0.17$, $\tilde{\beta}_{TC} = 0.82$, NO β_{TC} , $\beta_{QC} \approx 0.01$, $s \approx \beta_{QC}^{-1} = 100$
Comparison of (a)-(c), and (d)-(f), respectively, shows that s increases with increasing N and U .

$L_k(\beta)$ and $C(0, 0.8L)$ in Fig. 1. The system becomes practically phase coherent, as illustrated in Fig. 3(d), where $\sqrt{n_0 n_j} \approx G(0, j)$. For the parameter set in Figs. 1-3, we find that $\beta_{TC} \approx 0.115(5)$ which agrees with the analytical estimate $\tilde{\beta}_{TC} = [(U^2/6NV_t^2)^{1/3} \ln(9)] = 0.116$.

We now study the appearance of a phase-fluctuating condensate depending on the system parameters U , V_t , and N . The WI limit is characterized by $\gamma = U/2n \ll 1$. We define the average density by $n = N/2L$. Since we find that L equals L_{TF} within error bars in all cases, we use $\gamma = (3U^4/4V_t N^2)^{1/3}$. Note that the magnitude of γ in the inhomogeneous system differs from that in the homogeneous system. In Figs. 4(a)- 4(c), we demonstrate the effect of varying the number of particles N at on-site repulsion $U = 0.5$ and trapping $V_t = 0.01$. Both β_{QC} and β_{TC} decrease with increasing N , but since the change of β_{QC} is much greater than that of β_{TC} , the region of the phase-fluctuating condensate, $s = \beta_{TC}/\beta_{QC}$, increases with increasing N . The effect of varying U is illustrated in Figs. 4(d)- 4(f), where $N = 2000$ and $V_t = 0.4$. Increasing U , causes β_{QC} to decrease, while β_{TC} increases. Thus β_{TC}/β_{QC} grows with increasing U . More generally, the deeper we are in the Thomas-Fermi limit of large

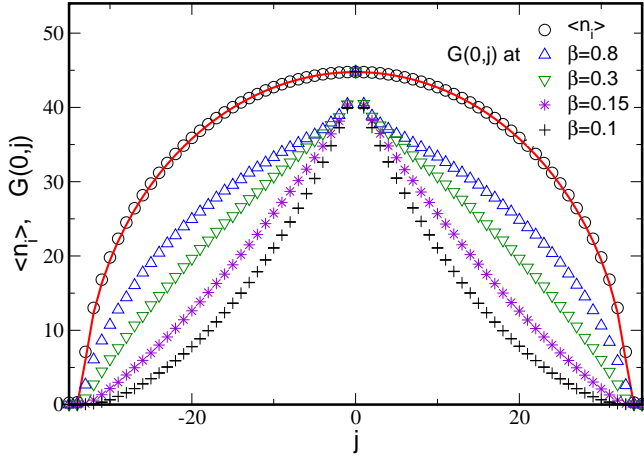


FIG. 5: (Color online) $N = 2000$, $U = 10.0$, $V_t = 0.4$ ($\gamma = 0.17$). The density profile $\sqrt{n_0 n_j}$ (\circ) is invariant for $\beta \geq \beta_{QC} \approx 0.1$, while the Green's function $G(0, j)$ varies throughout the QC regime. However, $G(0, j)$ does not approach $\sqrt{n_0 n_j}$ (as in Fig. 3). The line is a TF fit to $\sqrt{n_0 n_j}$ with $L = 33.3$ ($L_{TF} = 33.5$).

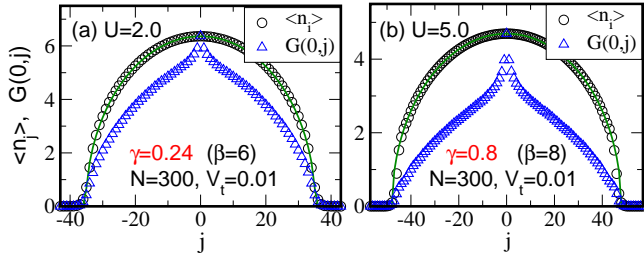


FIG. 6: (Color online) Ground state $\sqrt{n_0 n_j}$ (\circ) and $G(0, j)$ (Δ) for different γ . The lines are fits to a TF profile with (a) $L = 35.2$ ($L_{TF} = 35.6$) and (b) $L = 48.0$ ($L_{TF} = 48.3$). For increasing γ , the correlation hole becomes more pronounced, and thus the quantum depletion increases.

$\mu_{TF}/\hbar\omega \sim [(NU)^4/V_t]^{1/6}$, the larger is the size of the quasicondensate.

While for the parameter sets in Figs. 4(a)- 4(e), good agreement of $G(0, j)$ with expression (2) is observed for all β , as well as $\beta_{TC} \approx \tilde{\beta}_{TC}$, this does not apply to the example in Fig. 4(f), where $\gamma = 0.17$. Instead, $G(0, j)$ exhibits a qualitatively different behavior when approaching the ground state, as can be seen in Fig. 5: the phase-fluctuating condensate is beautifully realized, however, $G(0, j)$ does not approach $\sqrt{n_0 n_j}$ for $T \rightarrow 0$, and cannot be described by Eq. (2).

We consider the effect of stronger interactions in the trapped system on the phase-correlation properties in more detail. In Fig. 6, we show the ground state profiles for $N = 300$, $V_t = 0.01$, $U = 2.0$ and $U = 5.0$, respectively. We observe the same qualitative behaviour of the saturated Green's function as in Fig. 5. Close to the center of the cloud, where the density is higher, the decay of $G(0, j)$ is exponential; however, it broadens to-

ward the outer, more diluted regions of the cloud. By comparing Figs. 6(a) and 6(b), it can be seen that for larger γ , the correlation hole in the central region of the condensate is larger. Clearly, the quantum depletion for the parameter sets in Fig. 6 is much more significant than for systems in the WI limit, since the number of particles with zero momentum $N(k = 0) = \sum_{j,j'} G(j, j')/M$ decreases if $G(j, j') < \sqrt{n_j n_{j'}}$. We also observe this behavior if the density is smaller than 1 everywhere in the trap, and therefore exclude the possibility that it is an effect of the optical lattice. The shape of $G(0, j)$ is consistent with the two limiting cases, i.e. exponential decay in the strong-coupling limit, and phase-coherence [i.e. Eq.(2)] in the weak-coupling limit.

We conclude with a summary of our main results. In the mean-field, weakly interacting and Thomas-Fermi limits, both true a Thomas-Fermi condensate and a phase-fluctuating condensate emerge. Phase correlation properties, manifest in the characteristic decay of the single-particle density matrix, agree with surprising precision with the mean-field theory in [10]. In an intermediate-coupling regime, a true condensate no longer appears. The regime of the phase-fluctuating condensate persists even longer, extending to $T = 0$. We observe a qualitatively different decay of the Green's function, which cannot be accounted for by mean-field studies.

We acknowledge helpful discussions with Y. Castin, G. Shlyapnikov and T. Esslinger. This work was supported by a CNRS PICS grant (G.G.B. and F.H.) and the Swiss National Science Foundation. The simulations were performed on the Hreidar Beowulf cluster at ETH Zurich.

-
- [1] N.D. Mermin and H. Wagner, Phys. Rev. Lett. **22**, 1133 (1966).
 - [2] P.C. Hohenberg, Phys. Rev. **158**, 282 (1967).
 - [3] L.P. Pitaevskii and S. Stringari, J. Low. Temp. Phys. **85**, 377 (1991).
 - [4] J.W. Kane and L.P. Kadanoff, Phys. Rev. **155**, 80 (1967); J. Math. Phys. **6**, 1902 (1965).
 - [5] F.D.M. Haldane, Phys. Rev. Lett. **47**, 1840 (1981).
 - [6] L. Reatto and G.V. Chester, Phys. Rev. **155**, 88 (1967).
 - [7] M. Schwartz, Phys. Rev. B **15**, 1399 (1977).
 - [8] W. Ketterle and N.J. van Druten, Phys. Rev. A **54**, 656 (1996).
 - [9] D.S. Petrov, M. Holzmann, and G.V. Shlyapnikov, Phys. Rev. Lett. **84**, 2551 (2000); D.S. Petrov, G.V. Shlyapnikov, and J.T.M. Walraven, *ibid.* **87**, 050404 (2001).
 - [10] D.S. Petrov, G.V. Shlyapnikov, and J.T.M. Walraven, Phys. Rev. Lett. **85**, 3745 (2000).
 - [11] I. Bouchoule, K.V. Kheruntsyan, and G.V. Shlyapnikov, Phys. Rev. A **75**, 031606(R) (2007).
 - [12] C. Mora and Y. Castin, Phys. Rev. A **67**, 053615 (2004).
 - [13] D.L. Luxat and A. Griffin, Phys. Rev. A **67**, 043603 (2003).
 - [14] N.M. Bogoliubov, C. Malyshev, R.K. Bullough and J.

- Timonen, Phys. Rev. A **69**, 023619 (2004).
- [15] Yu. Kagan, B.V. Svistunov, and G.V. Shlyapnikov, Sov. Phys. JETP **66**, 480 (1987); Yu. Kagan, V.A. Kashurnikov, A.V. Krasavin, N.V. Prokof'ev, B.V. Svistunov, Phys. Rev. A **61**, 043608 (2000).
- [16] S. Dettmer *et. al.*, Phys. Rev. Lett. **87**, 160406 (2001); D. Hellweg *et. al.*, Appl. Phys. B: Lasers Opt. **73**, 781 (2001); S. Richard, F. Gerbier, J.H. Thywissen, M. Hugbart, P. Bouyer, and A. Aspect, *ibid.* **91**, 010405 (2003); J. Esteve, J.B. Trebbia, T. Schumm, A. Aspect, C.I. Westbrook, and O. Bouchoule, *ibid.* **96**, 130403 (2006); M. Hugbart *et. al.*, Europ. Phys. Jour. D **35**, 155 (2005).
- [17] E.H. Lieb and W. Liniger, Phys. Rev. **130**, 1605 (1963); E.H. Lieb, Phys. Rev. **130**, 1616 (1963).
- [18] D. Jaksch, C. Bruder, J.I. Cirac, C.W. Gardiner, and P. Zoller, Phys. Rev. Lett. **81** (1998) 3108.
- [19] F. D'Amico, S. Giorgini, L.P. Pitaevskii, and S. Stringari, Rev. Mod. Phys. **71**, 463 (1999).
- [20] S.M.A. Rombouts, K. van Houcke, and L. Pollet, Phys. Rev. Lett. **96**, 180603 (2006); K. van Houcke, S.M.A. Rombouts, and L. Pollet, Phys. Rev. E **73**, 056703 (2006).